Application of TEM: Dynamic changes of AKAP95-Cx43 complex during G1 phase of lung cancer cells

Zifeng Deng
State Key Laboratory of Molecular Vaccinology and Molecular Diagnositics, School of Public Health, Xiamen University

Rong Liu
State Key Laboratory of Molecular Vaccinology and Molecular Diganostics, School of Public Health, Xiamen University

Huiling Guo
State Key Laboratory of Molecular Vaccinology and Molecular Diagnostics, School of Public Health, Xiamen University

Luming Yao
State Key Laboratory of Celluar Stress Biology, School of Life Sciences, Xiamen University

FengKai Ruan
State Key Laboratory of Molecular Vaccinology and Molecular Diagnostics, School of Public Health, Xiamen University

Kai Wang
State Key Laboratory of Molecular Vaccinology and Molecular Diagnostics, School of Public Health, Xiamen University

Guihua Qiu
State Key Laboratory of Molecular Vaccinology and Molecular Diagnostics, School of Public Health, Xiamen University

Zhen Luo
State Key Laboratory of Molecular Vaccinology and Molecular Diagnostics, School of Public Health, Xiamen University

Guangping Luo
State Key Laboratory of Molecular Vaccinology and Mocular Diagnositcs, School of Public Health, Xiamen University

DongBei Guo
State Key Laboratory of Molecular Vaccinology and Molecular Diagnostics, School of Public Health, Xiamen University

Youliang Yao
State Key Laboratory of Molecular Vaccinology and Molecular Diagnostics, School of Public Health, Xiamen University

Yongxing Zhang (z63y94x@xmu.edu.cn)

Dalian University https://orcid.org/0000-0002-0887-9713

Research

Keywords: TEM, AKAP95-Cx43 complex, cyclin D1, cyclin E1, process of nuclear entry

Posted Date: September 8th, 2020

DOI: https://doi.org/10.21203/rs.3.rs-66232/v1

Abstract

Background

AKAP95(A-kinase anchoring protein) and Cx43 (connexin 43) express abnormally in lung cancer cells. As potential tumor therapeutic targets, specific process of bindings and dynamic changes of Cx43-AKAP95 complex in lung cancer cells may guide further treatments and detections of lung cancer. However, the process remains unclear now. We are aiming at investigating the dynamic changes of expression, localization, and binding of AKAP95 and Cx43, as well as their interaction with cyclin D1 and cyclin E1 in lung cancer cells during G1 phase.

Methods

A549 and Beas-2B cells were arrested at preliminary stage(P), middle stage(M) and restriction point(R) of G1 phase and Western blot(WB), Confocal laser scanning microscopy (CLSM) and Transmission electron microscope (TEM) were used in our study to detect proteins to provide further evidence of the correlation of these proteins.

Results: 1) AKAP95 carries Cx43 into the nucleus through the nuclear pore by binding to it during G1 phase. Some AKAP95 and Cx43 can aggregate and form larger protein aggregates. The process happens mainly during R stage. 2) AKAP95 and Cx43 mainly bind to cyclin D1 during P and M stage while bind to cyclin E1 during R stage respectively. Complexes of AKAP95-cyclin D1 and Cx43-cyclin D1 cannot enter nucleus while AKAP95-cyclin E1 and Cx43-cyclin E1 can.

Conclusions

1) Binding process of AKAP95-Cx43 complexes/ aggregates can be summarize as ‘bind and aggregate - target and enter nucleus- keep binding/aggregating in nucleus’. 2) Cyclin E1 was involved in the binding/aggregation and nuclear entry of AKAP95 and Cx43 while cyclin D1 only binds to them respectively in the cytoplasm.

Background

Aberrant expression of AKAP95 and Cx43 will lead abnormal cell cycle or even cause cancers [1-3]. Our previous studies have indicated that expression of AKAP95 increases while expression of Cx43 decreases in lung cancer, esophageal cancer etc. tissues [4-6]. The two proteins can bind to each other, correlating with cyclin Ds and Es. AKAP95 mainly promotes cell proliferation by up-regulate cyclin D1-3 and cyclin E1/2 and Cx43 down-regulates cyclin D1-3 and cyclin E1/2 to inhibit proliferation [7]. AKAP95-Cx43 complex can enter nucleus during G1 phase [8].

AKAP95 is the only protein which has been found that can enter nucleus of AKAPs family [9]. It has been reported that AKAP95 regulates transcription and promotes cell cycle etc. by targeting and binding to some proteins of nuclear membrane and nuclear matrix [10-15]. Recent studies have reported that a

single cluster of basic amino acids (SV40-like class of nuclear localization signal) influences nuclear entry of AKAP95and p68RNA helicases is related to AKAP95's ability to target the nuclear matrix [13,14]. AKAP95 also binds to nuclear pore complex protein to locate nuclear pore [15].

As a member of connexins family, Cx43 is a vital protein for gap junction communication of adjacent cells. Cx43 plays a variety of biological functions, including regulating proliferation, development, and differentiation etc. of cells [2,16,17]. Our foregoing study had suggested that AKAP95 might carry Cx43 into the nucleus [8] and the two proteins regulate cell cycle by interacting with cyclin D1-3 and cyclin E1/2 [5,7,18].

Restriction point (RP) determines whether the cell is proliferating [19,20]. Cyclin D1 and cyclin E1 are essential proteins for cells to complete G1/S conversion through RP [21,22]. After binding to CDK4/6, cyclin D1 can further promote the activation of cyclin E1/2-CDK2 [23,24], which is the vital regulators and effect target of E2Fs [25]. By promoting phosphorylation of retinoblastoma (Rb), cyclin E1/2 can promote the activation of E2Fs and G1/S conversion [21,24,25]. Though phosphorylation of retinoblastoma relies on cyclin D-CDK4 and cyclin E1-CDK2, cyclin D-CDK4 is relied earlier [15,25]. The non-phosphorylated Rb keeps binding to E2Fs, preventing DNA replication and transcription and leaving cells rest [19,20,22]. Our latest study had demonstrated that AKAP95 can up-regulate the expression of cyclin D1 and cyclin E1/2 while Cx43 can down-regulate them. AKAP95 and Cx43 can competitively bind to cyclin E1/2, regulating G1/S conversion [8]. In this study, G1 phase is further divided into three stages and TEM is used to detect binding and dynamic changes during G1 phase of above proteins in A549 cells.

Results

TEM images show that AKAP95 carries Cx43 into the nucleus through nuclear pore by binding with it during G1 phase.

Based on our foregoing work, A549 and Beas-2B cells were arrested at P, M and R stages which were treated with Lovastatin, Mimosine and Thymidine respectively in this article [26-29]. CLSM and TEM were used to analyze the expression and dynamic changes of their binding at different stages of G1 phase. Flow cytometry (FCM) was used to detect the effect of cell blocking and A549 groups were chosen to be detected. Results are shown in Fig.1A. After treated with Lovastatin and Mimosine respectively, proportion of cells in G1 phase increased while proportion of cells in G2 phase decreased. No significant changes were found of percentage of cells in S phase compared with the control group. Percentage of cells in G1 phase of Lovastatin group was higher than Mimosine group. In Thymidine group, which mainly arrests cells between late G1 and early phase, proportion of cells in S phase increased while proportion of cells in G1 phase decreased. No significant changes were found of percentage of cells in G2 phase compared with the control group (Fig.1Aa). Fig1.Ab shows the bar chart of the statistical results of Fig.1Aa. These data show that cells were arrested in P, M, and R stage efficiently.

WB was used to detect expression of AKAP95 and Cx43 in arrested cells. Fig.1B shows the results. In A549 cells, both AKAP95 and Cx43 had low level expression during P and M stages, but highly expressed

in R stage (Fig.1Ba). Statistical results of protein expression in different stages are shown in Fig.1Bb. Both expression of AKAP95 and Cx43 in these three stages was different respectively ($p < 0.05$), and both of their expression increased gradually form P to R stage and peaked at R stage (Fig.1Bb). In Beas-2B cells (normal lung tissue cells), AKAP95 expressed much lower than that in A549 cells or Cx43 in Bease-2B cells (Fig.1Bc). Both AKAP95 and Cx43 in Beas-2B cells highly expressed form M stage, which was earlier than that in A549 cells, and kept highly expression (Fig.1Bd). The results that the expression of AKAP95 increased while expression of Cx43 decreased in tumor cells were consistent with our previous research [5-7]. In Both A549 and Beas-2B cell lines, expression of AKAP95 had showed the same trend, suggesting correlation between them.

Images of CLSM show that AKAP95 mainly expressed in nucleus during whole G1 phase and no significant cytoplasmic expression was found in arrested cells. In addition, some strong fluorescent patches could be found in nucleus, suggesting that some AKAP95 aggregated with each other and form protein aggregates. Cx43 expressed both in nucleus and cytoplasm during whole G1 phase and equably located in cells. These data were consistent with our previous work [18].

Gold labeled IgG in different diameters were used to label AKAP95(15nm) and Cx43(10nm) and TEM was used to detect gold labels in cells to show binding of AKAP95 and Cx43 at P, M, and R stage. We have firstly provided the TEM images that AKAP95 binds to Cx43 and carried it into nucleus through nuclear pore at the subcellular level. It is generally considered that two proteins bind to each other when the distance of gold labels of them is less than 15nm in TEM images [30,31]. In Fig.2A, the green triangle points to AKAP95 (15nm label) and the red triangle points to Cx43 (10nm label). The distance of the two label is less than 15nm (take the scale on the picture as the standard), suggesting that AKAP95 can bind to Cx43. Fig.2B shows that AKAP95-Cx43 complex just enter nucleus through nuclear pore. The green and red triangle points to AKAP95 and Cx43 respectively and the blue arrow refers to the nuclear membrane. The nuclear pore is between the two arrows on the right of the image (the interval marked by the red line).

Dynamic process of AKAP95-Cx43 complex entering nucleus.

This article had further observed the dynamic changes of binding of AKAP95 and Cx43, as well as the process of entering nucleus of AKAP95-Cx43 complex by TEM. 15nm and 10nm Gold labeled IgG were used to mark AKAP95 and Cx43 respectively and the locations and bindings of AKAP95-Cx43 complexes/ aggregates in cells at P, M, and R stage were detected.

In TEM assay, different concentrations of gold labeled IgG may affect the results. When the dilution ratio of Gold labeled IgG was 1:100, a few gold particles showed nonspecific adhesion causing false positive while when the dilution ratio was 1:100, though false positive could be avoided, some target proteins could not be labeled and displayed caused by low concentration of gold labeled IgG. In order to verify whether there was false positive interference under our experimental conditions, Rabbit anti- and Mouse anti-GAPDH were used to incubated sections before incubation with Gold labeled IgG (15nm and 10nm) in Positive Control while PB buffer was used instead of specific GAPDH antibodies in Negative Control group. Fig.3A shows that gold labels could be found in Positive control and distance of different labels

was significantly more than 15nm (Fig.3Aa) while only extremely few gold labels were found in Negative Control groups, and no nonspecific aggregation were found (Fig.3Ab, 3Ac), suggesting that the false positive interference could be ignored under our experimental condition. Statistical results of Fig.3A is shown in Fig.3B: Average distance of different gold labels of Control (Positive Control in Fig. 3Aa) group was more than 100nm and no nonspecific adhesion or aggregation had been detected while it was less than 10nm in groups that cells arrested at P, M, and R stages, suggesting that our results were reliable. In our subsequent assays, we used a dilution ratio of 1:100 of Gold labeled IgG to show the general law of distribution and position of proteins, and 1:1000 to show location and constituents of single protein complex.

Images of binding and location of AKAP95 and Cx43 at different stages of G1 phase are shown in Fig.3C (A549 cells) and Fig.3D (Beas-2B cells). We found that binding of AKAP95 and Cx43 could be detected at P (Fig.3Ca), M (Fig.3Cb), and R (Fig.3Cc) stage and complexes of AKAP95 and Cx43 could be detected in nucleus at all these three stages. Due to the low expression of AKAP95 and Cx43 at P stage, only a few AKAP95- Cx43 complex were formed and entered nucleus. That mainly happened at M and R stages when both AKAP95 and Cx43 expressed more. This finding was different from our previous report that AKAP95 and Cx43 can bind and enter nucleus only at late G1 phase [1]. The reason might be that TEM is much more sensitive, compared with Co-IP/WB and IF. In addition, protein aggregation of AKAP95 and Cx43 was detected in our assay, suggesting that some AKAP95 and Cx43 proteins aggregated with each other and formed bigger protein aggregates. The aggregates existed in both nucleus and cytoplasm (Fig.3C, in red circle), suggesting that the protein aggregates had the ability of entering nucleus as well and kept aggregating after nucleus entry. In Beas-2B cells, binding of AKAP95 and Cx43 could also be found both in nucleus and cytoplasm, which was similar with that in A549 groups, suggesting that AKAP95 and Cx43 could bind and enter nucleus both in normal and tumor cells at P, M, and R stage. Thus, AKAP95 and Cx43 in A549 cells were chosen to be detected in our subsequent assays.

Fig.3 TEM images of AKAP95-Cx43 complex at different stages of G1 phase in arrested A549 and Beas-2B cells. Dilution ratio of Gold labeled IgG was 1:100. Blue arrows point into nucleus and the border of strong refraction is nuclear membrane. (A) a. Image of Positive Control. b. Image of Negative Control. c. Image of nonspecific adhesion of gold label of Negative Control. (B) Statistical results of distance of gold labels with different diameters of different groups. Scales on each TEM images were chosen to be standard and distance of 10 pairs of 15nm and 10nm gold labels in each group were detected. Distances of 15nm and 10nm gold labels that marks GAPDH were analyzed in control (Positive Control in Fig.3B) and distances of 15nm and 10nm gold labels that marks AKAP95 and Cx43 respectively were analyzed in Lovastatin, Mimosine, and Thymidine groups. (C) Images of binding and location of AKAP95-Cx43 complexes in arrested A549 cells. Green triangles point to AKAP95 and red triangles point to Cx43(10nm). Protein aggregates of AKAP95 and Cx43 are marked by red circles. (D) Images of binding and location of AKAP95-Cx43 complexes in arrested Beas-2B cells. Green triangles point to AKAP95 and red triangles point to Cx43(10nm). Protein aggregates of AKAP95 and Cx43 are marked by red circles.

In Fig.4, images of various location of AKAP94-Cx43 complexes/aggregates in different stages of the process of nucleus entry are shown. a. AKAP95 bound to Cx43 in cytoplasm. b. Complex/aggregates located near nuclear membrane (still in cytoplasm). c. Complex/aggregates located on the nuclear membrane. d. Complex/aggregates located near nuclear membrane (in nucleus). e. Complexes of AKAP95-Cx43 kept binding in nucleus. f. Aggregates of AKAP95-Cx43 kept aggregating in nucleus.

Fig.4 TEM images of the location of nucleus entry process of AKAP95-Cx43 complexes/aggregates. Images of A549 cells were chosen to show the process of binding and entering nucleus of AKAP95-Cx43 complexes/aggregates. Dilution ratio of Gold labeled IgG was 1:100. Blue arrows point into nucleus and the border of strong refraction is nuclear membrane. Green triangles point to AKAP95 and red triangles point to Cx43(10nm). Protein aggregates of AKAP95 and Cx43 are marked by red circles.

2.3 AKAP95 and Cx43 bind to cyclin D1 and cyclin E1 in G1 phase.

AKAP95 and cyclin D1 were correlated in lung cancer tissues. We had found that AKAP95 and Cx43 can bind cyclin D1/D2 while can competitively bind cyclin E1/E2 respectively, regulating the G1/S conversion [7,32-34]. In this article, we have provided detection results of binding and dynamic changes of AKAP95, Cx43, cyclin D1 and cyclin E1 at P, M, R stages during G1 phase of lung cancer cells.

Expressions of AKAP95, Cx43, cyclin D1, and cyclin E1 of cells arrested at P, M, and R stages were detected (Fig.5A). The results showed that cyclin D1 highly expressed at P and S stages while lowly expressed at R stage (Fig.5Aa, the third row). The expression of cyclin D1 during G1 phase gradually declined and there was statistical significance in each group (Fig.5Ab $p<0.05$). Expressions of cyclin E1 were low at P and M stages while peaked at R stage during G1 phase (Fig.5Aa, the fourth row). Compared to expressions P and M stage, increase of expression of cyclin E1 at R stages was statistically significant (Fig.5Ab $p<0.05$). Specific AKAP95 and Cx43 antibodies were used in Co-IP assay to detect protein combinations of the total protein from P, M, and R stage cells. Both cyclin D1 and cyclin E1 can be detected in coprecipitation in Co-IP: AKAP95 group (Fig.5B), suggesting that AKAP95 correlated with cyclin D1 and cyclin E1 during whole G1 phase. Similar results were found in Co-IP: Cx43 group (Fig. 5C), suggesting that Cx43 correlated with cyclin D1 and cyclin E1 during whole G1 phase as well. These results suggest us that AKAP95, Cx43, cyclin D1, and cyclin E1 could bind to each other and formed at least four complexes, including AKAP95-cyclin D1, AKAP95-cyclin E1, Cx43-cyclin D1, Cx43-cyclin E1, during G1 phase. Due to the difference of expression level of the four proteins mentioned above at P, M, and R stage during G1 phase, we considered that AKAP95-cyclin D1 and Cx43-cyclin D1 mainly existed at P and M stage while AKAP95-cyclin E1 and Cx43-cyclin E1 were formed mainly at R stage of G1 phase.

Fig.5 A549 Expressions and bindings of AKAP95, Cx43, cyclin D1, and cyclin E1 during G1 phase in A549 cells. Total proteins were extracted from arrested A549 cells and WB assay was used to detect expression levels of AKAP95, Cx43, cyclin D1, and cyclin E1 in different groups. (A) a. Expression of AKAP95, Cx43, cyclin D1, and cyclin E1 at P, M, R stages. b. Statistical results of Fig.5Aa. (B) Results of Co-IP: AKAP95 assay of arrested A549 cells. (C) Results of Co-IP: Cx43 assay of arrested A549 cells.

Locations of cyclin D1 and cyclin E1 at different stages in cells were detected by CLSM and TEM. Results of CLSM had shown that cyclin D1 mainly expressed at P and M stage, and its expression level decreased significantly at R stage. No significant intracellular expression of cyclin D1 was found during whole G1 phase in CLSM images (Fig.6Aa, the second row). Cyclin E1 mainly expressed at R stage and obvious intracellular expression and protein aggregation could be detected at this stage. During the other two stages, cyclin E1 expressed weakly and mainly located in cytoplasm (Fig.6Ab, the second row). TEM images showed location of cyclin D1 and cyclin E1 in cell at the subcellular level. Gold labels which marked cyclin D1 can be detected during whole G1 phase, but except for a few labels close to the nuclear membrane, no labels can be found in nucleus at all three staged of G1 phase (Fig.6B). However, gold labels that marked cyclin E1 can be detected both in nucleus and cytoplasm in images of P, M, and R stage cells, and significant protein aggregation could be found, especially in R stage cells (Fig.6C). These results were consistent with data of CLSM.

Fig.6 Distribution of cyclin D1and cyclin E1 in P, M, and R stage A549 cells. (A) Slides of arrested A549 cells treated were incubated with specific cyclin D1 and cyclin E1 antibodies (1:100) respectively. a. The first row shows images of DAPI□The second row shows images of cyclin D1 at different stages□The third row shows merge images of DAPI and cyclin D1. b. The first row shows images of DAPI□The second row shows images of cyclin E1 at different stages□The third row shows merge images of DAPI and cyclin E1. (B) Dilution ratio of Gold labeled IgG was 1:100. Blue arrows point into nucleus and the border of strong refraction is nuclear membrane. Green triangles point to cyclin D1. (C) Dilution ratio of Gold labeled IgG was 1:100. Blue arrows point into nucleus and the border of strong refraction is nuclear membrane. Green triangles point to cyclin E1. Protein aggregate of cyclin E1 is marked by red circles.

Under the condition that dilution ratio of Gold labeled IgG was 1:1000, we had further detected the location of AKAP95-cyclin D1, AKAP95-cyclin E1, Cx43-cyclin D1, and Cx43-cyclin E1 complexes/aggregates in P, M, and R stage cells respectively. The results are shown in Fig.7. During G1 phase, AKAP95, cyclin D1 and their complexes were localized in cytoplasm and no significant protein aggregation was found (Fig.7A). Binding of AKAP95 and cyclin E1 could be detected both in. Significant protein aggregation of cyclin E1 were found both in nucleus and cytoplasm as well (Fig.7B). Binding of Cx43 and cyclin D1 could be detected in cytoplasm at P and M stage, but image of their binding at R stage was not found this time. No significant protein aggregation was found (Fig.7C). Binding of Cx43 and cyclin E1 can be observed both in nucleus and cytoplasm at P, M, and R stage and significant protein aggregation of Cx43 and cyclin E1 were detected (Fig.7D).

Fig.7 Images of binding and location of AKAP95-cyclin D1, Cx43-cyclin D1, AKAP95-cyclin E1, and Cx43-cyclin E1 at P, M, and R stage. Dilution ratio of Gold labeled IgG was 1:1000. Blue arrows point into nucleus and the border of strong refraction is nuclear membrane. (A) Green triangles point to cyclin D1(15nm) and red triangles point to AKAP95(10nm). (B) Green triangles point to cyclin E1(15nm) and red triangles point to AKAP95(10nm). Protein aggregates of AKAP95 and cyclin E1 are marked by red circles. (C) Green triangles point to cyclin D1(15nm) and red triangles point to Cx43(10nm). (D) Green triangles

point to cyclin E1(15nm) and red triangles point to Cx43(10nm). Protein aggregates of Cx43 and cyclin E1 are marked by red circles.

Discussion

In normal lung cells, Cx43 highly expressed while expression of AKAP95 extremely low. However, expression of AKAP95 significantly increased and expression of Cx43 decreased in lung cancer cells. Abnormal expression of these two proteins may be one of important reasons of lung cancer formation. Our article had shown that the difference of expression of these two proteins between normal and cancerous lung cells happened from early G1 phase.

Binding and nuclear entry of AKAP95-Cx43 complexes/aggregates happens both in normal and cancerous lung cells. Based on our previous work, we further divide G1 phase into three stages, and use TEM with higher resolution to detect the binding of AKAP95 and Cx43 during G1 phase at the subcellular level. More intuitive evidence is provided and binding and dynamic changes of AKAP95-Cx43 complex/aggregate are analyze in this article. We conclude the process as:1) AKAP95 can bind to Cx43 and carry it into nucleus during whole G1 phase, not only at late G1 phase. Some AKAP95 and Cx43 can form protein aggregates. 2) AKAP95 targets the nuclear membrane, guiding the AKAP95-Cx43 complexes/aggregates move towards the nuclear membrane. 3) After locating on the nuclear membrane, AKAP95 continues to target the nuclear matrix, guiding AKAP95-Cx43 complexes/aggregates entering nucleus through nuclear pore. AKAP95-Cx43 complexes/aggregates keep binding/aggregating in nucleus. 4) Process mentioned above happens in the whole G1 phase (P, M, and R), but mainly at R phase when they highly express.

According to our data, AKAP95□Cx43□cyclin D1 and cyclin E1 can form at least four complexes/ aggregates, including AKAP95-cyclin D1 and Cx43-cyclin D1, which cannot enter nucleus, and AKAP95-cyclin E1and Cx43-cyclin E1, which can be detected both in nucleus and cytoplasm.

At P and M stage, cyclin D1 highly expresses and binds to AKAP95 and Cx43 respectively. AKAP95 inhibits the degradation of cyclin D1, which can promote the activation of cyclin E1 and inhibit the inhibitory effect of p21 and p27 on cyclin E-DCK2 activity by binding to it while Cx43 binds to cyclin D1 promoting its degradation [7,35]. Both AKAP95-cyclin D1 and Cx43 cyclin D1 locate only in cytoplasm at these two stages. AKAP95 and Cx43 can bind to each other to prevent the other one binding to cyclin D1[7]. At R stage, cyclin D1 lowly expresses. According to our data, the process happened only in cytoplasm.

During whole G1 phase, AKAP95-Cx43, AKAP95-cyclin E1, and Cx43-cyclin E1 complexes/aggregates can enter nucleus, especially at R stage when these three proteins highly express. AKAP95 and Cx43 can bind to cyclin E1 competitively [7]. Binding of AKAP95 and cyclin E1 promotes the G1/S conversion by promoting hypo- and hyper- phosphorylation of Rb while Cx43 promotes the degradation of cyclin E1 and phosphorylation of Rb by binding to cyclin E1[7,18]. In addition, AKAP95 and Cx43 can bind to each other

to inhibit each other's binding to cyclin E1, regulating the function of cyclin E1 and G1/S conversion [7]. According to our data, the process happened both in nucleus and cytoplasm.

Interestingly, significant AKAP95-Cx43, AKAP95-cyclin E1, and Cx43-cyclin E1 aggregates were found in TEM images while AKAP95-cyclin D1 and Cx43-cyclin D1 aggregates were not detected. Aggregates of AKAP95-Cx43, AKAP95-cyclin E1, and Cx43-cyclin E1 could enter nucleus through nuclear pore while AKAP95-cyclin D1 and Cx43-cyclin D1 could not. We consider that cyclin D1 is not involved in protein aggregation of AKAP95, Cx43, and cyclin E1. However, significance of these aggregates remains unclear and further work is needed to clarify it.

Together with our foregoing data [5,7,18], we conclude the dynamic changes of correlation of AKAP95, Cx43, cyclin D1 and cyclin E1 as:1) At P and M stages, AKAP95-cyclin D1 and Cx43-cyclin D1 complexes are mainly formed. These complexes do not enter the nucleus and function in cytoplasm. 2) At R stage, AKAP95, Cx43, and cyclin E1 highly express and mainly form AKAP95-Cx43, AKAP95-cyclin E1, and Cx43-cyclin E1 complexes/aggregates. These complexes/aggregates can be targeted into nucleus by AKAP95 and maintain binding or aggregating in the nucleus, promoting G1/S conversion.

Conclusion

In normal lung cells, Cx43 highly expressed while expression of AKAP95 extremely low. However, expression of AKAP95 significantly increased and expression of Cx43 decreased in lung cancer cells. Abnormal expression of these two proteins may be one of important reasons of lung cancer formation. Our article had shown that the difference of expression of these two proteins between normal and cancerous lung cells happened from early G1 phase.
Binding and nuclear entry of AKAP95-Cx43 complexes/aggregates happens both in normal and cancerous lung cells. Based on our previous work, we further divide G1 phase into three stages, and use TEM with higher resolution to detect the binding of AKAP95 and Cx43 during G1 phase at the subcellular level. More intuitive evidence is provided and binding and dynamic changes of AKAP95-Cx43 complex/aggregate are analyze in this article. We conclude the process as:1) AKAP95 can bind to Cx43 and carry it into nucleus during whole G1 phase, not only at late G1 phase. Some AKAP95 and Cx43 can form protein aggregates. 2) AKAP95 targets the nuclear membrane, guiding the AKAP95-Cx43 complexes/aggregates move towards the nuclear membrane. 3) After locating on the nuclear membrane, AKAP95 continues to target the nuclear matrix, guiding AKAP95-Cx43 complexes/aggregates entering nucleus through nuclear pore. AKAP95-Cx43 complexes/aggregates keep binding/aggregating in nucleus. 4) Process mentioned above happens in the whole G1 phase (P, M, and R), but mainly at R phase when they highly express.
According to our data, AKAP95□Cx43□cyclin D1 and cyclin E1 can form at least four complexes/aggregates, including AKAP95-cyclin D1 and Cx43-cyclin D1, which cannot enter nucleus, and AKAP95-cyclin E1and Cx43-cyclin E1, which can be detected both in nucleus and cytoplasm.
At P and M stage, cyclin D1 highly expresses and binds to AKAP95 and Cx43 respectively. AKAP95 inhibits the degradation of cyclin D1, which can promote the activation of cyclin E1 and inhibit the

inhibitory effect of p21 and p27 on cyclin E-DCK2 activity by binding to it while Cx43 binds to cyclin D1 promoting its degradation [7,35]. Both AKAP95-cyclin D1 and Cx43 cyclin D1 locate only in cytoplasm at these two stages. AKAP95 and Cx43 can bind to each other to prevent the other one binding to cyclin D1[7]. At R stage, cyclin D1 lowly expresses. According to our data, the process happened only in cytoplasm.
During whole G1 phase, AKAP95-Cx43, AKAP95-cyclin E1, and Cx43-cyclin E1 complexes/aggregates can enter nucleus, especially at R stage when these three proteins highly express. AKAP95 and Cx43 can bind to cyclin E1 competitively [7]. Binding of AKAP95 and cyclin E1 promotes the G1/S conversion by promoting hypo- and hyper- phosphorylation of Rb while Cx43 promotes the degradation of cyclin E1 and phosphorylation of Rb by binding to cyclin E1[7,18]. In addition, AKAP95 and Cx43 can bind to each other to inhibit each other’s binding to cyclin E1, regulating the function of cyclin E1 and G1/S conversion [7]. According to our data, the process happened both in nucleus and cytoplasm.
Interestingly, significant AKAP95-Cx43, AKAP95-cyclin E1, and Cx43-cyclin E1 aggregates were found in TEM images while AKAP95-cyclin D1 and Cx43-cyclin D1 aggregates were not detected. Aggregates of AKAP95-Cx43, AKAP95-cyclin E1, and Cx43-cyclin E1 could enter nucleus through nuclear pore while AKAP95-cyclin D1 and Cx43-cyclin D1 could not. We consider that cyclin D1 is not involved in protein aggregation of AKAP95, Cx43, and cyclin E1. However, significance of these aggregates remains unclear and further work is needed to clarify it.
Together with our foregoing data [5,7,18], we conclude the dynamic changes of correlation of AKAP95, Cx43, cyclin D1 and cyclin E1 as:1) At P and M stages, AKAP95-cyclin D1 and Cx43-cyclin D1 complexes are mainly formed. These complexes do not enter the nucleus and function in cytoplasm. 2) At R stage, AKAP95, Cx43, and cyclin E1 highly express and mainly form AKAP95-Cx43, AKAP95-cyclin E1, and Cx43-cyclin E1 complexes/aggregates. These complexes/aggregates can be targeted into nucleus by AKAP95 and maintain binding or aggregating in the nucleus, promoting G1/S conversion.

Abbreviations

A-kinase anchoring protein-AKAP95; connexin 43-Cx43; preliminary stage of G1 phase-P; middle stage of G1 phase-M; restriction point-R; Western blot-WB; Confocal laser scanning microscopy-CLSM; Transmission electron microscope-TEM; Flow cytometry-FCM.

Materials And Methods

Antibodies

Mouse anti-AKAP95(sc-100643), anti-Cx43(sc-13558), anti-cyclin D2(sc-53637), anti-cyclin D3(sc-6283), anti-cyclin E2 (sc-28351) were purchased from Santa Cruz (Texas, USA); Mouse anti-Cx43(ab79010), Rabbit anti-AKAP8(ab134923), anti-Cx43(ab235586), anti-cyclin D1(ab134175), anti-cyclin D2(ab207604), anti-cyclin D3(ab28283), anti-cyclin E1(ab33911), anti-cyclin E2(ab40890) were purchased from Abcam(Cambridge, UK); Mouse anti GADPH(T0004), Rabbit anti-AKAP8(AF0333), anti-Cx43(AF0137), anti-GADPH(AF7021) were purchased from Affnity Biosciences(Ohio, USA)Goat Anti-

rabbit IgG/Gold (AB-0295G-Gold, 15 nm), Goat Anti-mouse IgG/Gold (AB-0296R-Gold, 10 nm) were purchased from Leading Biology Inc. (California, USA);Goat Anti-rabbit IgG FITC(HA1004), Goat Anti-mouse IgG H&L TRITC(HA1017) were purchased from Hangzhou HuaAn Biotechnology Co., Ltd (Hangzhou, China).

Reagents

Protein A/G Plus-Agarose(sc-2003) were purchased from Santa Cruz(Texas, USA)，Lovastatin, Mimosine, DAPI, Antifade Solution and Cell Cycle and Apoptosis Analysis Kit were purchased from Dalian Meilun Biotechnology Co., Ltd (Dalian, China); Thymidine was purchased from Solarbio(Beijing, China); Western Lab Peroxidase (E1050) were purchased from Beijing LABLEAD BIOTECH (Beijing, China).

Cell culture and protein extraction

A549 and Beas-2B cells culture: A549 and Beas-2B cells lines were preserved in our laboratory. Cells were cultured in DMEM medium (containing 10% fetal bovine serum) under the conditions of 5% CO2, 90% humidity ,37℃. Lovastatin (0.015 μmol/mL，, Mimosine，0.004 μmol/mL，,and Thymidine，0.003 μmol/mL， was added into the medium and cultured for 24h when cells needed to be arrested. Total proteins were extracted using RIPA/p0013 buffer from synchronous cells.

Co-Immunoprecipapation

Add 5μg primary antibody to every 500μg total protein. After incubated by a shaker at 4℃ overnight(8h), add 20μl Protein A/G plus-agarose and keep incubation for another 8 hours. Collect the supernatant after centrifugation (3000 rpm), then wash the coprecipitate 2-3 times by PBS buffer. Lysate (RIPA/p0013 buffer) was used to resuspend and dissolve coprecipitate. The protein (coprecipitate and supernatant) can be detected or stored at -20℃ after boiled. Add Loading buffer to protein before boiling.

Western Blot

Add 50μg protein sample to per hole of SDS-PAGE gel. Electrophoresis was performed under 120 V constant pressure and protein was transferred on PVDF membranes at a constant current of 300mA. Membranes were incubated with specific primary antibodies overnight (8h) at 4℃ after incubated with skimmed milk powder for 1h. Membranes were then incubated with IgG antibodies at 37℃ for 1 hour. Proteins were detected by BIO RAD Chemi DOC XRS+ Imaging System and bands of proteins were analyzed using Image Lab. Bands of GAPDH or Input group were used to normalize the date of other groups.

Statistical analysis

IBM SPSS Statistics 20(SPSS Inc., Chicago, IL, USA) was used to analyze statistics. Data was compared using independent t- test and ，<0.05 was considered significant. Statistical charts were exported by GraphPad Prism8.

Flow cytometry

Cells were collected by centrifugation (3000rpm) and fixed with 75% ethanol at 4℃ for 18-24 hours. Cell cycle detection kit was used to stain cells and stained cells should be washed using PBS buffer 1-2 times before detection using flow cytometry (Beckman CytoFLEX). FlowJo V10 was used to analyze data.

Immunofluorescence

Slides were taken out when cell density reach 60%-80%. Slides were fixed with 4% paraformaldehyde for 1 hour and incubated with 1% BSA for 30 minutes. Under the 4℃ condition, slides were incubated with specific primary antibodies overnight (8h) before incubated with fluorescent IgG antibodies for 1 hour at 37℃. After stain cells with DAPI and add quenching agent to slides, confocal laser scanning microscopy (Olympus FV1200) was used to observe cells. Images were analyzed by FV10-ASW 4.2 Viewer.

Immunoelectron microscopy

Centrifuge(3000rpm) and collect cells, and then fix cells with 4% paraformaldehyde for 2-3 hours at 4℃. After washed by PB buffer (0.0162M Na_2HPO_3+0.038M NaH_2PO_3) for 3 times, gradient concentration of ethanol was used in the dehydration of cells. Cells were embedded by LR White resin and were sliced after that. The slides were sealed by 1% BSA for 15-20 minutes at room temperature and incubated with specific primary antibodies overnight (8 hours) at 4℃. PB buffer was used to wash slides for 3 times (5 minutes for each time), and after that, under 37℃ condition, slides were incubated with Gold labeled IgG antibodies for 1 hour at 37℃. Wash slides for 3 times (5 minutes for each time). Slides then had been fixed by 2.5% glutaraldehyde and washed by PB buffer for 3 times (3 minutes for each time). After stained with uranium and lead, slides were detected and photographed by transmission electron microscope (Tecnai G2 Spirit BioTwin).

Declarations

Ethics approval and consent to participate

Not applicable.

Consent for publication

Not applicable.

Availability of data and materials

Data available.

Competing interests

No inflect of interests of this article.

Funding

This research was funded by National Natural Science Foundation of China (No.81071927& No.31741006), the Natural Science Foundation of Fujian Province of China (No. 2016J01407), XMU Training Program of Innovation and Entrepreneurship for Undergraduates (No.20720192016), Innovation Practice Platform for Undergraduates Students, School of Public Health Xiamen University (No.202004&No.202005).

Authors' contributions

ZD and YZ contributed to study design; ZD and RL were the main operators; HG, LY and FR provided methodological help; KW, GQ, ZL and GL helped with the software; DG and YL provided some equipment support; ZD wrote the article and YZ revised the article.

Acknowledgements

Not applicable.

References

1. Decrock E, De Vuyst E, Vinken M et al. Connexin 43 hemichannels contribute to the propagation of apoptotic cell death in a rat C6 glioma cell model. Cell Death Differ. 2009,16(1):151-163.
2. Lezcano V, Bellido T, Plotkin LI et al. Role of connexin 43 in the mechanism of action of alendronate: Dissociation of anti-apoptotic and proliferative signaling pathways. Archives of Biochemistry and Biophysics. 2012,518(2):95-102.
3. Johnstone SR, Best AK, Wright CSet al. Enhanced connexin 43 expression delays intra-mitoitc duration and cell cycle traverse independently of gap junction channel function. Cell Biochem. 2010,110(3):772-782.
4. Wenzhi Liu, Suhang Hua, Yue Dai et al. Roles of Cx43 and AKAP95 in ovarian cancer tissues in G1/S phase. Int J Clin Exp Pathol. 2015,8(11):14315–14324.
5. ShuoWang, KaiWang, Zifeng Deng et al. Correlation between the protein expression levels of A-kinase anchor protein95, p-retinoblastoma (Ser780), cyclin D2/3, and cyclin E2 in esophageal cancer tissues. Asia-Pac J Clin Oncol. 2019,1–5.
6. Zhiyu Guan, Winxin Zhuang, Hui Lei et al. Epac1, PDE4, and PKC protein expression and their correlation with AKAP95 and Cx43 in esophagus cancer tissues. Thoracic Cancer. 2017,8:572–576.
7. Renzhen Chen, Yu Chen, Yangyang Yuan et al. Cx43 and AKAP95 regulate G1/S conversion by competitively binding to cyclin E1/E2 in lung cancer cells. Thoracic Cancer. 2020,11:1594–1602
8. Xiaoxuan Chen, Xiangyu Kong, Wenxin Zhuang et al. Dynamic changes in protein interaction between AKAP95 and Cx43 during cell cycle progression of A549 cells. Sci Rep. 2016, 6:21224.

9. Jing Hu, Alireza Khodadadi-Jamayran, Miaowei Mao et al. AKAP95 regulates splicing through scaffolding RNAs and RNA processing factors. Nat Commun. 2016,7:13347.
10. Wong, W. and Scott, J. D. AKAP signalling complexes: focal points in space and time. Nat. Mol. Cell Biol. 2004,5:959–970.
11. Yun Li, Gary D Kao, Benjamin A Garcia et al. A novel histone deacetylase pathway regulates mitosis by modulating Aurora B kinase activity. Genes Dev. 2006,20:2566–2579.
12. Jungmann, R. A. and Kiryukhina, O. Cyclic AMP and AKAP-mediated targeting of protein kinase A regulates lactate dehydrogenase subunit A mRNA stability. J. Biol. Chem. 2005,280:25170–25177.
13. L Akileswaran, J W Taraska, J A Sayer et al. A-kinase-anchoring Protein AKAP95 Is Targeted to the Nuclear Matrix and Associates With p68 RNA Helicase. J Biol Chem 2001,276 (20):17448-17454.
14. Hicks G. R., Raikhel N.V. Protein Import Into the Nucleus: An Integrated View. Annu. Rev. Cell Dev. Biol. 1995,11:155–188.
15. Graciela López-Soop, Torunn Rønningen, Agnieszka Rogala et al. AKAP95 interacts with nucleoporin TPR in mitosis and is important for the spindle assembly checkpoint. Cell Cycle 2017,16 (10):947-956.
16. Decrock E, De Vuyst E, Vinken M et al. Connexin 43 hemichannels contribute to the propagation of apoptotic cell death in a rat C6 glioma cell model. Cell Death Differ. 2009,16(1):151-163.
17. Bruzzone R. Learning the language of cel-cell communication through connexin channels. Genome Biol. 2001,2(11): 4027.1-4027.5.
18. Xiangyu Kong, Dengcheng Zhang, Wenxin Zhuang et al. AKAP95 promotes cell cycle progression via interactions with cyclin E and low molecular weight cyclin E. Am J Transl Res. 2016,8(2):811-826.
19. Riaan Conradie, Frank J. Bruggeman, Andrea Ciliberto et al. Restriction point control of the mammalian cell cycle via the cyclin E/Cdk2: p27 complex. FEBS Journal 2010,277: 357–367.
20. Planas-Silva MD and Weinberg RA. The restriction point and control of cell proliferation. Current Opin. Cell Biol. 1997, 9:768–772.
21. Johannes Boonstra. Progression Through the G1-Phase of the On-Going Cell Cycle. Journal of Cellular Biochemistry. 2003,90:244–252.
22. Irina Neganova and Majlinda Lako. G1 to S phase cell cycle transition in somatic and embryonic stem cells. Journal of Anatomy. 2008,213:30-44.
23. Ignacio Perez-Roger, Soo-Hyun Kim, Beatrice Griffiths et al. Cyclins D1 and D2 mediate Myc-induced proliferation via sequestration of $p27^{Kip1}$ and $p21^{Cip1}$. The EMBO Journal. 1999,18 (19) :5310–5320.
24. Ylva HEDBERG, Estela DAVOODI, Bo¨rje LJUNGBERG et al. Cyclin E and P27 protein content in human renal cell carcinoma: clinical outcome and associations with cyclin D. Int. J. Cancer. 2002,102:601–607.
25. Rory Donnellan and Runjan Chetty. Cyclin E in human cancers. The FASEB Journal. 1999,13:773-780.
26. JAN LAMPRECHT, CEZARY WÓJCIK, MAREK JAKÓBISIAK et al. Lovastatin induces mitotic abnormalities in various cell lines. Cell Biology International. 1999,23(1):51–60.

27. Paul A. Watson, Hartmut H. Hanauske-Abel, Alan Flint et al. Mimosine Reversibly Arrests Cell Cycle Progression at the G1-S Phase Border. Cytometry. 1991,12:242-246.
28. Lalande M. A reversible arrest point in the late G1 phase of the mammalian cell cycle. Exp Cell Res.1990,186:332-339.
29. Cooper, K. Z. Chen and S. Ravi. Thymidine block does not synchronize L1210 mouse leukaemic cells: implications for cell cycle control, cell cycle analysis and whole-culture synchronization. Cell Prolif. 2008,41:156-167.
30. Scott R. Johnstone, Brett M. Kroncke, Adam C. Straub et al. MAPK Phosphorylation of Connexin 43 Promotes Binding of Cyclin E and Smooth Muscle Cell Proliferation. Circ Res. 2012,111:201-211.
31. Neetu M. Gulati, Udana Torian, and John R. Gallagher et al. Immunoelectron Microscopy of Viral Antigens. Current Protocols in Microbiology. 2019,53-86.
32. Arsenijevic T, Degraef C, Dumont JE et al. A novel partner for D-type cyclins: protein kinase A-anchoring protein AKAP95. Biochemical Journal. 2004,378(2):673-679.
33. Zhao S, Yi M, Yuan Y, et al. Expression of AKAP95, Cx43, cyclinE1 and cyclinD1 in esophageal cancer and their association with the clinical and pathological parameters. International Journal of Clinical and Experimental Medicine. 2015,8(5):7324-7332.
34. Matsushime H, Quelle DE, Shurtleff SA et al. D-type cyclin-dependent kinase activity in mammalian cells. Mol Cell Biol. 1994,14(3):2066-2076.
35. Dean Smith, David Mann and Kwee Yong. Cyclin D type does not influence cell cycle response to DNA damage caused by ionizing radiation in multiple myeloma tumours. British Journal of Haematology. 2016,173:693–704.

Figures

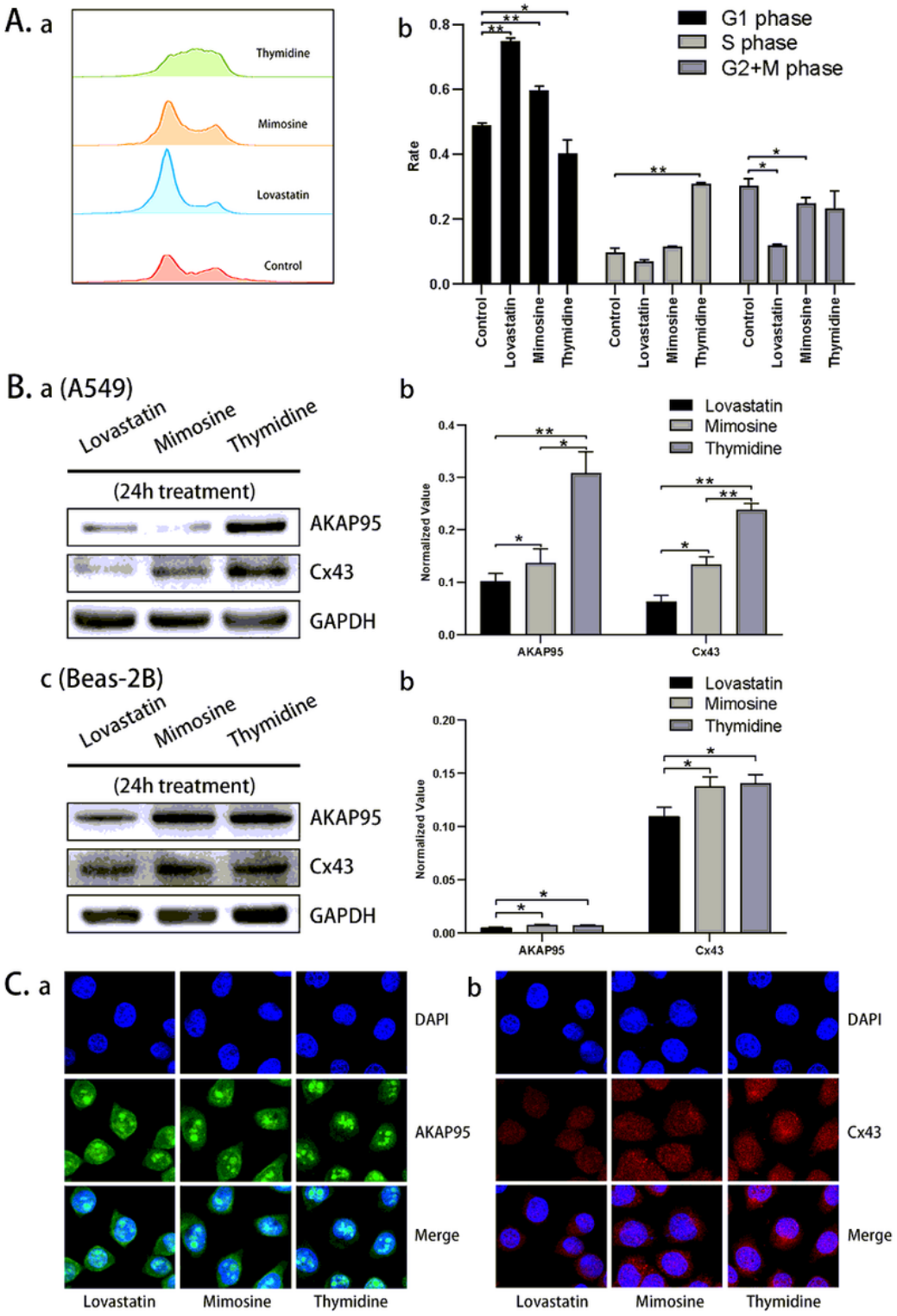

Figure 1

Detection of cell cycle after arresting and expression of AKAP95 and Cx43 in A549 and Beas-2B cells. (A) FCM was used to detect phases of arrested A549 cells. Cells of control group were treated without drugs. (B)Total proteins were extracted from arrested A549 and Beas-2B cells and detected by WB. Loading 50μg protein per lane and dilution ratio of specific antibodies was 1:3000. Gray value of GAPDH band was used to normalized data. The ratio of gray value of AKAP95 and Cx43 band to GAPDH band was

used as variable for statistical analysis among groups (* means p<0.05; **means p<0.01). Each experiment was repeated three time. (C) Slides of arrested A549 cells were incubated with specific AKAP95 and Cx43 antibodies (1:100) respectively. After incubated with IgG (FITC) and IgG (TRITC) respectively and stained by DAPI, CLSM was used to detect cells. Images were export by FV10-ASW 4.2 Viewer. a. The first row shows images of DAPI，The second row shows images of AKAP95 at different stages，The third row shows merge images of DAPI and AKAP95. b. The first row shows images of DAPI， The second row shows images of Cx43 at different stages，The third row shows merge images of DAPI and Cx43.

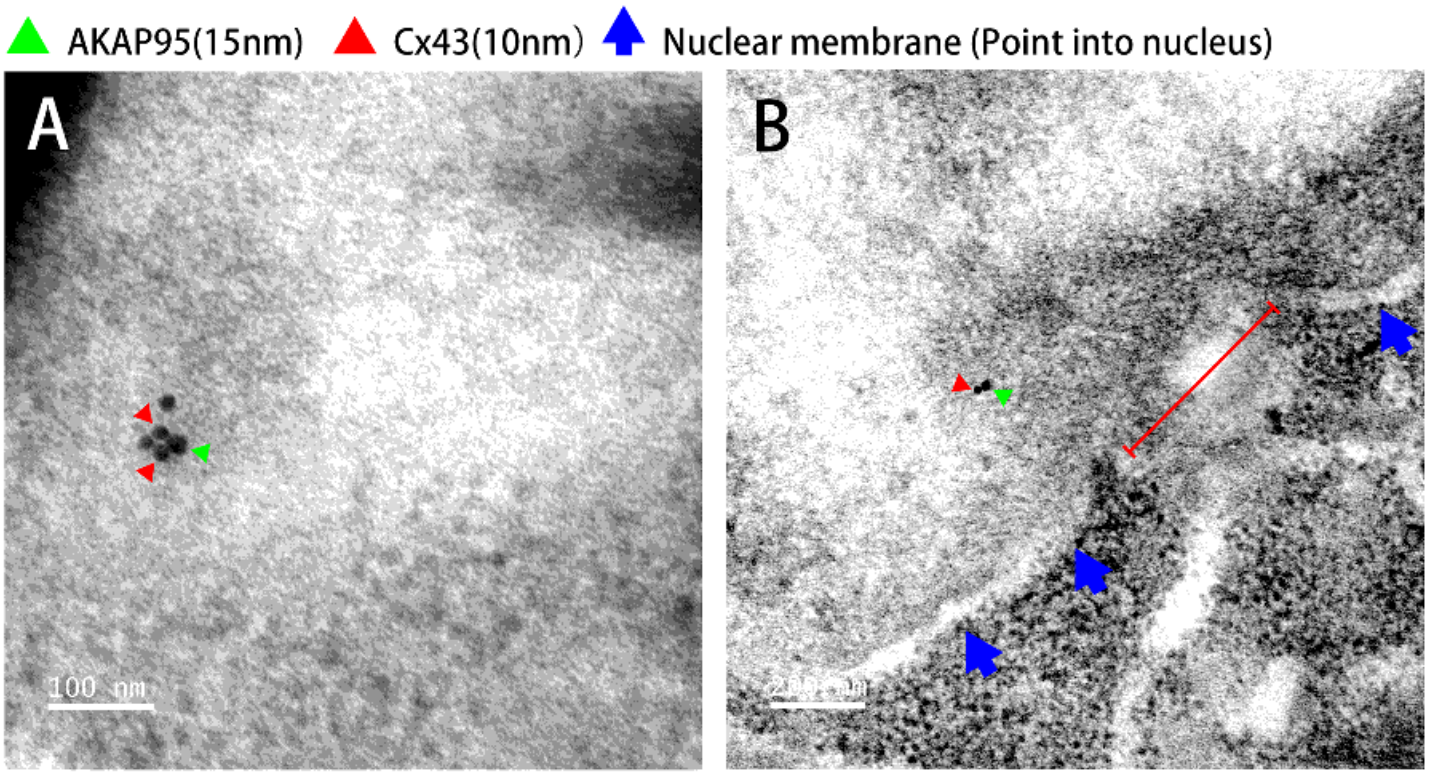

Figure 2

TEM images of binding of AKAP95 and Cx43 in A549 cells. Arrested cells were fixed by 4% paraformaldehyde and embedded in paraffin. After sectioning, cells were sealed with 1% BSA and incubated with specific antibodies（1:100）and Gold labeled IgG (1:1000). Sections then stained by lead and uranium. TEM (Tecnai G2 Spirit BioTwin) was used to catch images. Blue arrows point into nucleus and the border of strong refraction is nuclear membrane. The nuclear membrane fault shown by the red line is the nuclear pore. (A)AKAP95 binds to Cx43. (B)AKAP95-Cx43 complex enter nucleus through nuclear pore.

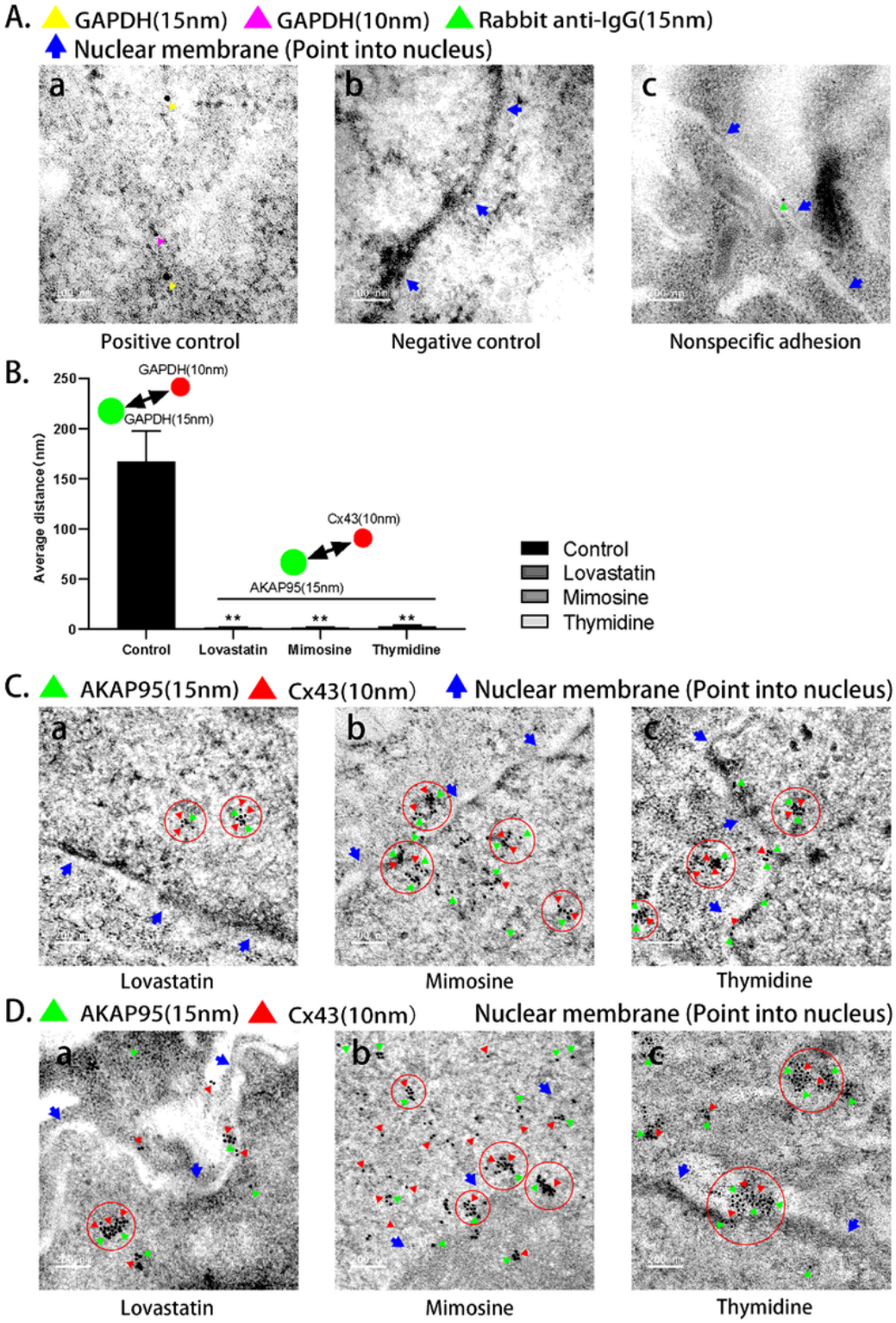

Figure 3

TEM images of AKAP95-Cx43 complex at different stages of G1 phase in arrested A549 and Beas-2B cells. Dilution ratio of Gold labeled IgG was 1:100. Blue arrows point into nucleus and the border of strong refraction is nuclear membrane. (A) a. Image of Positive Control. b. Image of Negative Control. c. Image of nonspecific adhesion of gold label of Negative Control. (B) Statistical results of distance of gold labels with different diameters of different groups. Scales on each TEM images were chosen to be standard and

distance of 10 pairs of 15nm and 10nm gold labels in each group were detected. Distances of 15nm and 10nm gold labels that marks GAPDH were analyzed in control (Positive Control in Fig.3B) and distances of 15nm and 10nm gold labels that marks AKAP95 and Cx43 respectively were analyzed in Lovastatin, Mimosine, and Thymidine groups. (C) Images of binding and location of AKAP95-Cx43 complexes in arrested A549 cells. Green triangles point to AKAP95 and red triangles point to Cx43(10nm). Protein aggregates of AKAP95 and Cx43 are marked by red circles. (D) Images of binding and location of AKAP95-Cx43 complexes in arrested Beas-2B cells. Green triangles point to AKAP95 and red triangles point to Cx43(10nm). Protein aggregates of AKAP95 and Cx43 are marked by red circles.

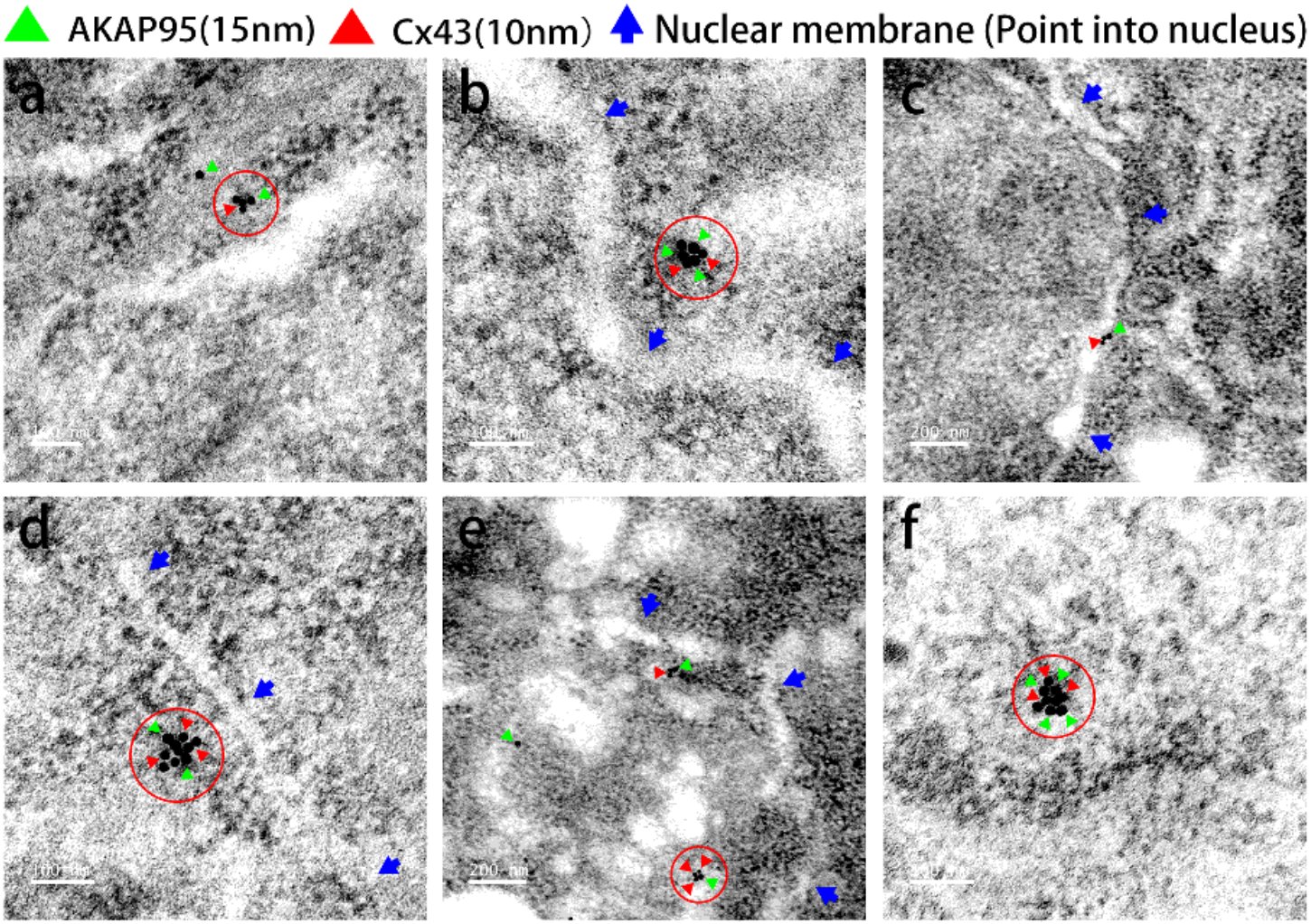

Figure 4

TEM images of the location of nucleus entry process of AKAP95-Cx43 complexes/aggregates. Images of A549 cells were chosen to show the process of binding and entering nucleus of AKAP95-Cx43 complexes/aggregates. Dilution ratio of Gold labeled IgG was 1:100. Blue arrows point into nucleus and the border of strong refraction is nuclear membrane. Green triangles point to AKAP95 and red triangles point to Cx43(10nm). Protein aggregates of AKAP95 and Cx43 are marked by red circles.

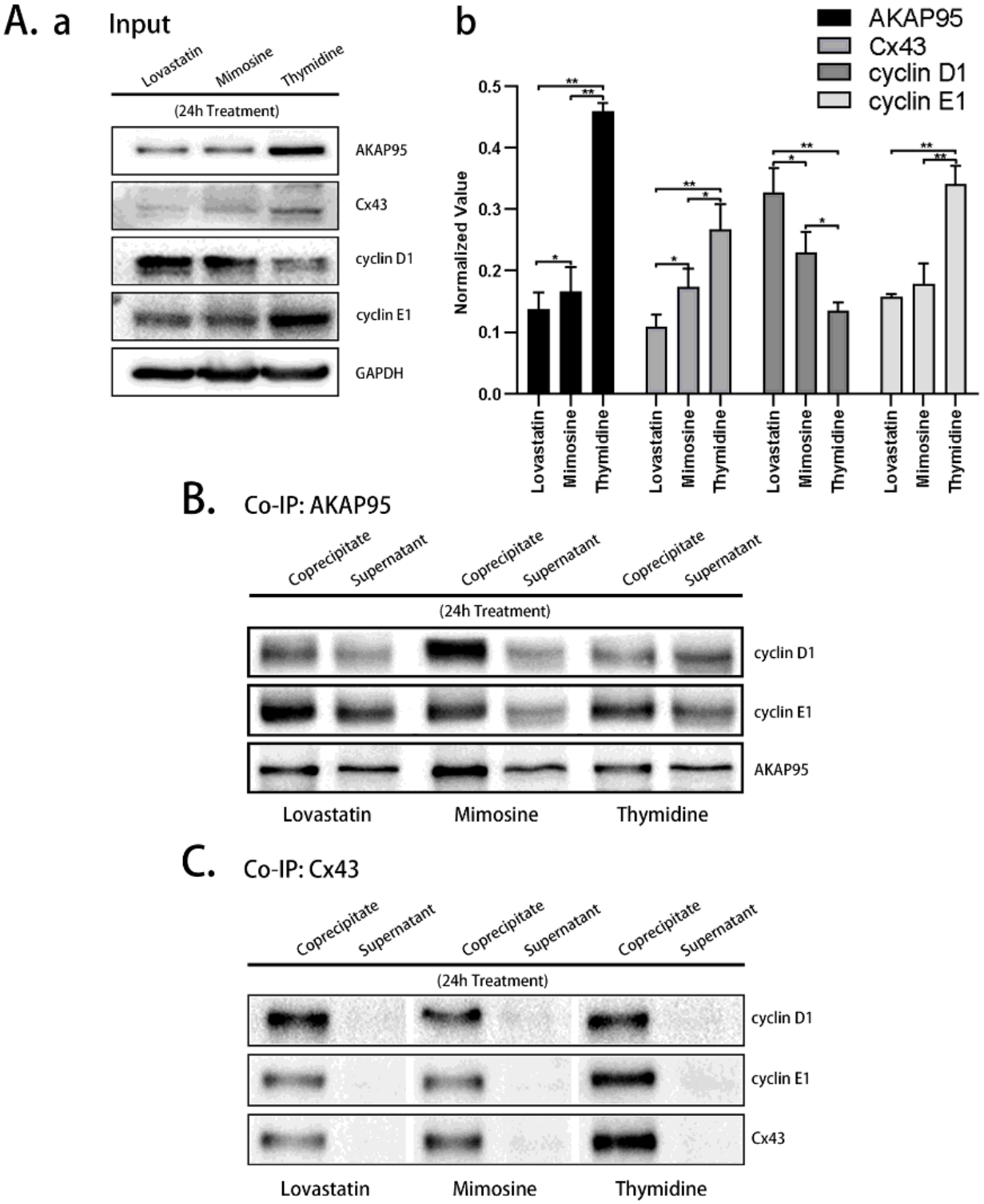

Figure 5

A549 Expressions and bindings of AKAP95, Cx43, cyclin D1, and cyclin E1 during G1 phase in A549 cells. Total proteins were extracted from arrested A549 cells and WB assay was used to detect expression levels of AKAP95, Cx43, cyclin D1, and cyclin E1 in different groups. (A) a. Expression of AKAP95, Cx43, cyclin D1, and cyclin E1 at P, M, R stages. b. Statistical results of Fig.5Aa. (B) Results of Co-IP: AKAP95 assay of arrested A549 cells. (C) Results of Co-IP: Cx43 assay of arrested A549 cells.

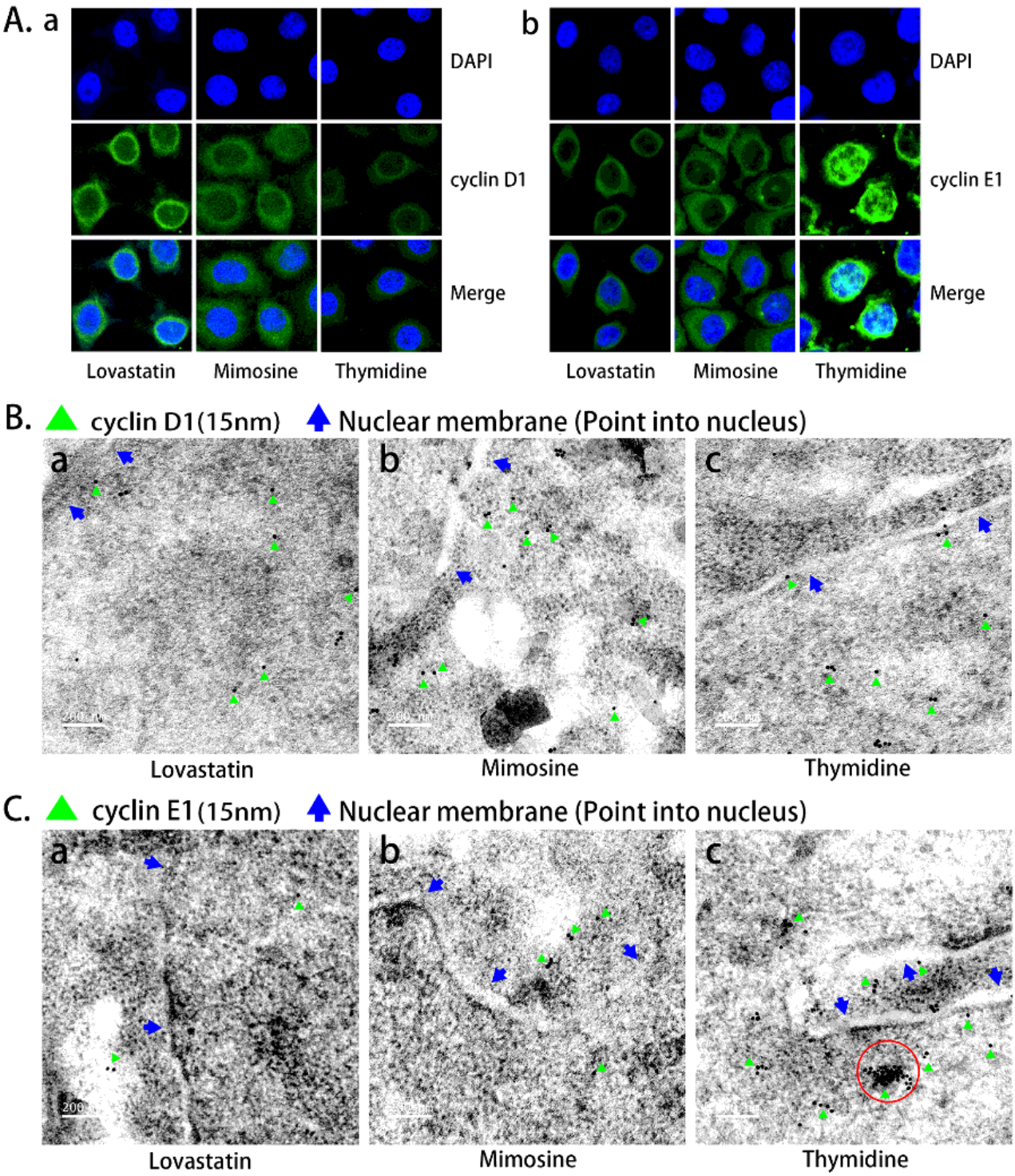

Figure 6

Distribution of cyclin D1and cyclin E1 in P, M, and R stage A549 cells. (A) Slides of arrested A549 cells treated were incubated with specific cyclin D1 and cyclin E1 antibodies (1:100) respectively. a. The first row shows images of DAPI The second row shows images of cyclin D1 at different stages The third row shows merge images of DAPI and cyclin D1. b. The first row shows images of DAPI The second row shows images of cyclin E1 at different stages The third row shows merge images of DAPI and cyclin E1.

(B) Dilution ratio of Gold labeled IgG was 1:100. Blue arrows point into nucleus and the border of strong refraction is nuclear membrane. Green triangles point to cyclin D1. (C) Dilution ratio of Gold labeled IgG was 1:100. Blue arrows point into nucleus and the border of strong refraction is nuclear membrane. Green triangles point to cyclin E1. Protein aggregate of cyclin E1 is marked by red circles.

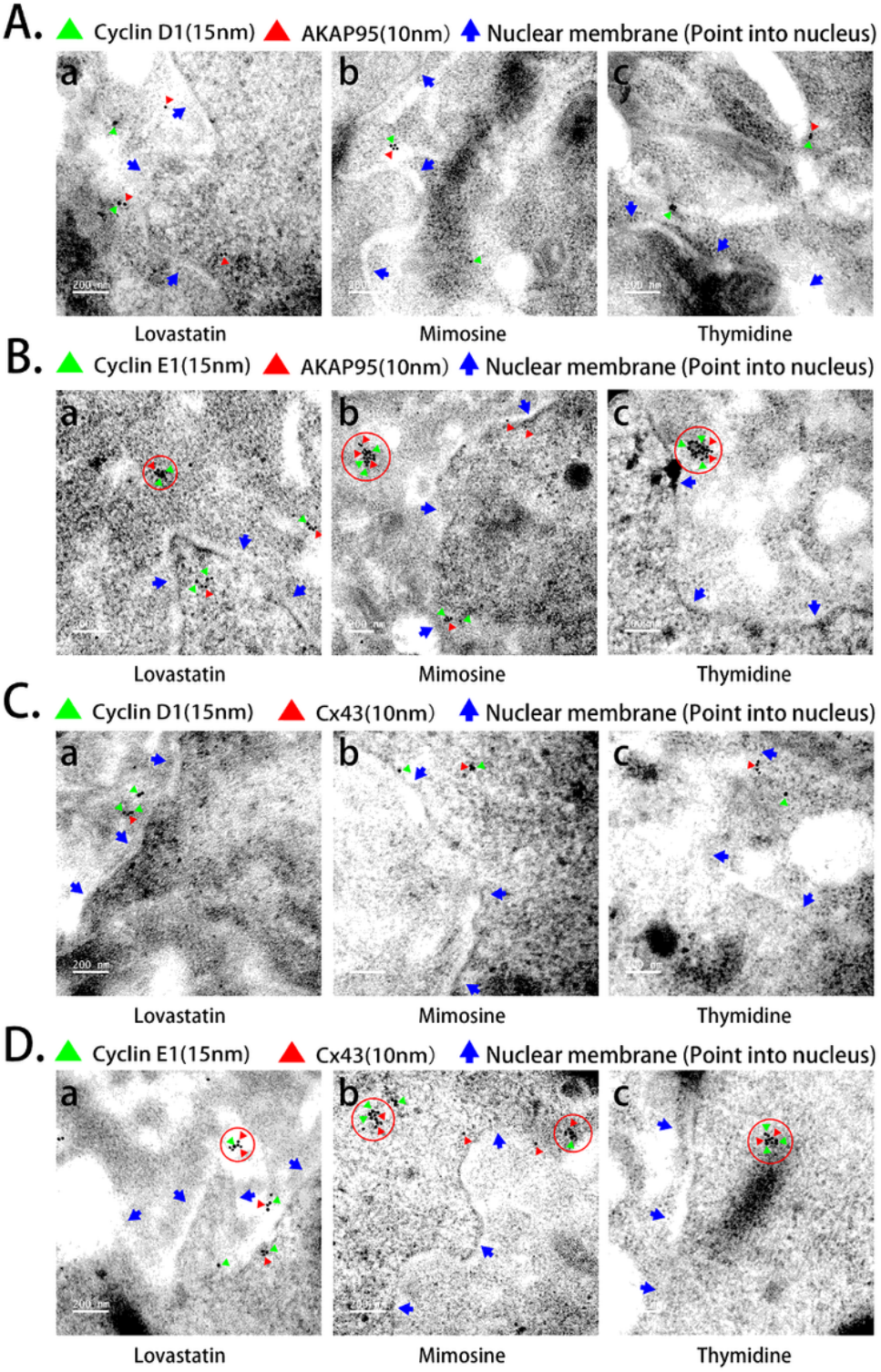

Figure 7

Images of binding and location of AKAP95-cyclin D1, Cx43-cyclin D1, AKAP95-cyclin E1, and Cx43-cyclin E1 at P, M, and R stage. Dilution ratio of Gold labeled IgG was 1:1000. Blue arrows point into nucleus and the border of strong refraction is nuclear membrane. (A) Green triangles point to cyclin D1(15nm) and red triangles point to AKAP95(10nm). (B) Green triangles point to cyclin E1(15nm) and red triangles point to AKAP95(10nm). Protein aggregates of AKAP95 and cyclin E1 are marked by red circles. (C) Green triangles point to cyclin D1(15nm) and red triangles point to Cx43(10nm). (D) Green triangles point to cyclin E1(15nm) and red triangles point to Cx43(10nm). Protein aggregates of Cx43 and cyclin E1 are marked by red circles.